

Fabrication of Bottom Free Magnetic Tunnel Junctions for Bio-Magnetic Field Sensor Application

Kosuke Fujiwara¹, Mikihiro Oogane¹, Takuo Nishikawa², Hiroshi Naganuma¹ and Yasuo Ando¹

¹Department of Applied Physics, Graduate School of Engineering, Tohoku University,
Aoba-yama 6-6-05, Sendai 980-8579, Japan

Phone: +81-022-795-7949 E-mail: fujiwara@mlab.apph.tohoku.ac.jp

²LC Business Department, KONICA MINOLTA TECHNOLOGY CENTER, INC.
No.1 Sakura-machi, Hino-shi, Tokyo 191-8511, Japan

1. Introduction

Since large tunnel magneto-resistance (TMR) effect at room temperature (RT) in magnetic tunnel junctions (MTJs) [1,2] spurred intensive investigation of MTJ applications for spin-electronics devices, such as magnetic random access memory (MRAM) and various magnetic field sensors (read heads of hard disk drive, micro compasses) [3,4]. For sensor application, low power consumption of MTJs makes and small device size them prime candidate of the next generation magnetic field sensor. However, the sensitivity has been limited, because MTJs with amorphous Al-Oxide barriers exhibit relatively small TMR ratios below 100%. The TMR ratio has been improved dramatically by developing the (001)-oriented MgO barriers, over 200% were observed at RT [5,6,7]. These high TMR ratios enable us to design highly sensitive magnetic field sensors, such as bio-magnetic field sensor. In such applications, we need MTJs with a large sensitivity and linear resistance responses. For example, a high sensitivity of over 10%/Oe is required in individual MTJ for the bio-magnetic sensor consisting 100x100 integrated MTJs to achieve enough output signal and good S/N ratio [8]. Here, sensitivity is defined as $\text{TMR-ratio}/2H_k$, where H_k is anisotropy field.

In this study, we fabricated MTJs with an antiferromagnetic coupled NiFe (t_{NiFe}) / Ru (0.9) / CoFeB (3) (in nm) bottom free layers. In this trilayer [9], the magnetization of NiFe and CoFeB are strongly coupled by the middle thin Ru layer. In addition, we carried out double annealing process to achieve hysteresis-free linear resistance responses against external magnetic fields.

2. Experiment

The MTJs were deposited on to thermally oxidized Si(001) wafers using an ultrahigh vacuum ($P_{\text{base}} < 3 \times 10^{-6}$ Pa) magnetron sputtering system. The stacking structure was Sub. / Ta (5) / Ru (10) / Ta (5) / $\text{Ni}_{80}\text{Fe}_{20}$ (t_{NiFe}) / Ru (0.9) / $\text{Co}_{40}\text{Fe}_{40}\text{B}_{20}$ (3) / MgO (2.5) / $\text{Co}_{40}\text{Fe}_{40}\text{B}_{20}$ (3) / Ru (0.9) / $\text{Co}_{75}\text{Fe}_{25}$ (5) / $\text{Ir}_{22}\text{Mn}_{78}$ (10) / Ta (8) (in nm). The thickness of NiFe layer (t_{NiFe}) was 10, 20, 70, 150 and 200 nm. The bottom synthetic layers showed strong antiferromagnetic coupling and good thermal stability against the annealing below 325°C. The MTJs were micro-fabricated by conventional photolithography process, and the top pinned layers were patterned into $80 \times 40 \mu\text{m}^2$.

After microfabrication, the MTJs were annealed at 325°C for 1 h in a high vacuum furnace (first annealing). This first annealing was carried out with applied magnetic field of 300 Oe to the easy direction of the free layer in order to provide induced magnetic anisotropy. After the first annealing, MTJs were annealed again for 20 min in air with in-plane 90° rotated field of 100 Oe, which is the magnetic hard axis direction of the free layer. The second annealing provides the rotation of easy axis of the top pinned layer to the magnetic field direction (without the rotation of easy axis of the bottom free layer). In this condition, each easy axis of the bottom free and the top pinned are orthogonal, so the R - H minor curve reflects the M - H curve for hard direction of the bottom free layer, applying a magnetic field to easy axis of the top pinned layer.

The magnetoresistance properties were measured at RT using DC four probes with applied magnetic field swept with a 0.1 Oe step. The direction of the field was same as the hard axis of free layer. Noise measurements were performed in a magnetic shield room and MTJ noise was digitized and processed using a vector signal analyzer to obtain the noise power spectral density (S_v^2).

3. Result and Discussion

Figure 1 shows magnified views of R - H curves around zero fields for the MTJs with 70-nm-thick NiFe ($t_{\text{NiFe}} = 70$ nm) and various second annealing temperature ($T_{2\text{nd}}$). We found that the shape of the curves significantly changed with increasing $T_{2\text{nd}}$. For low $T_{2\text{nd}}$ (240°C and 260°C), the R - H curves showed hysteresis. For $T_{2\text{nd}} = 280^\circ\text{C}$ and 300°C , the curves without hysteresis have been observed, and very high sensitivity of 19.3%/Oe ($T_{2\text{nd}} = 280^\circ\text{C}$) and 25.3%/Oe ($T_{2\text{nd}} = 300^\circ\text{C}$) has been successfully achieved. This sensitivity enables us to detect bio-magnetic field by integration of the MTJs. Such high sensitivity permits us to detect pico-tesla region field as a signal of nano-volt. On the other hand, in high $T_{2\text{nd}}$ region ($T_{2\text{nd}} = 320^\circ\text{C}$ and 330°C), the curves shows some resistance jumps. Such resistance jumps are not suitable for sensor applications, because these are origins of error in actual sensor devices.

In above experiments, we found that linear hysteresis-free resistance response and maximum sensitivity were observed $T_{2\text{nd}} = 300^\circ\text{C}$, so in the following, we fixed 300°C as second annealing temperature and investigated t_{NiFe}

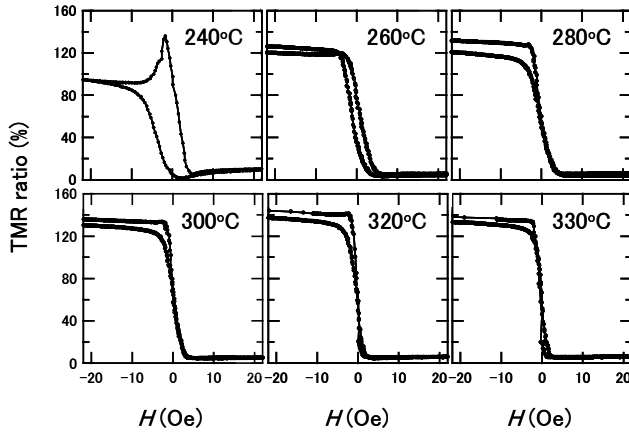


Fig. 1. Magnified R - H curve around zero field of MTJs with $t_{\text{NiFe}} = 70$ nm. The temperatures in figure are indicating $T_{2\text{nd}}$.

dependence. Figure 2 shows t_{NiFe} dependence of the TMR ratio (a), anisotropy field (H_k) (b), and value of sensitivity (TMR-ratio/ $2H_k$) (c). The TMR ratio gradually decreased with increased t_{NiFe} . This behavior is due to the inhibition of B atoms diffusion into Buffer Ta layer. Contrary H_k values drastically decreased with increasing t_{NiFe} . We believe that this changes result from the reduction of demagnetizing field in NiFe layers. As a result of t_{NiFe} dependence of TMR ratio and H_k , the sensitivity exhibited a peak around $t_{\text{NiFe}} = 70$ nm.

Figure 3 shows noise power spectrum density (S_v^2) of MTJ with $t_{\text{NiFe}} = 70$ nm and $T_{2\text{nd}} = 300^\circ\text{C}$ at different bias voltage in parallel magnetization state. The $1/f$ noise dominates the low-frequency region and its magnitude increases with increasing applied bias voltage as Hooge's formula [10]. In sensor-type MTJs, the detectivity, the conditions to which signal voltage becomes larger than noise voltage, D ($D = S_v / \text{Sensitivity}$) defines ideal minimum detectable field. In this study, the detectivity D was 4.2×10^{-6} Oe/Hz $^{1/2}$ at 40 mV bias voltage and 10 Hz. Such value permits us to detect bio-magnetic field with constituting 100x100 integrated MTJs.

Acknowledgements

This work was supported by S-Innovation program, Japan Science and Technology Agency (JST).

References

- [1] T. Miyazaki and N. Tezuka, J. Magn. Magn. Mater. **139** (1995) L231.
- [2] J. S. Moodera, L. R. Kinder, T. M. Wong and R. Meservey, Phys. Rev. Lett. **74** (1995) 3273.
- [3] K. S. Moon, Y. Chen and Y. Huai, J. Appl. Phys. **91** (2002) 7965.
- [4] F. Kou, M. Oogane and Y. Ando, J. Magn. Soc. Jpn. **32** (2008) 361.
- [5] S. Yuasa, T. Nagahama, A. Fukushima, Y. Suzuki and K. Ando Nat. Mater. **3** (2004) 868.
- [6] S. S. P. Parkin, C. Kaiser, A. Panchula, P. M. Rice, B. Hughes, M. Samant and A. H. Yang, Nat. Mater **3** (2004) 862.

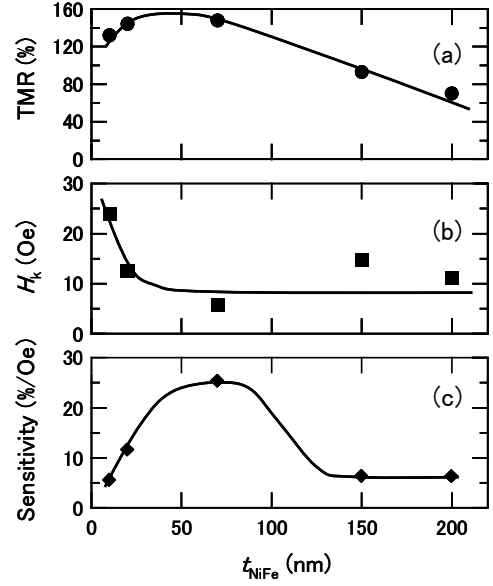


Fig. 2. t_{NiFe} dependence of TMR ratio (a), anisotropy field (H_k) (b), and Sensitivity (TMR-ratio/ $2H_k$) (c). All data were evaluated from magnetoresistance properties.

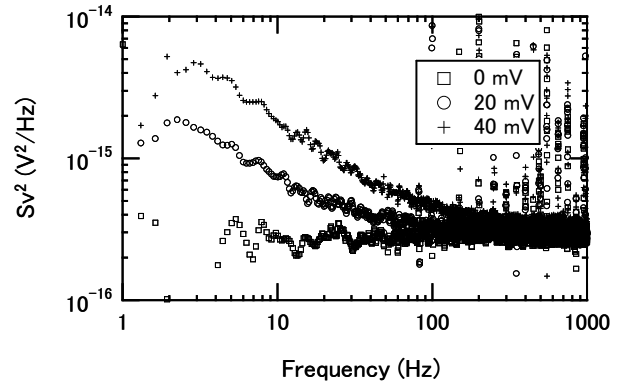


Fig. 3. Noise power spectrum density S_v^2 of MTJ with $t_{\text{NiFe}} = 70$ nm and $T_{2\text{nd}} = 300^\circ\text{C}$ at several bias voltage in parallel magnetization state.

- [7] D. D. D. Djayaprawora, K. Tsunekawa, M. Nagai, H. Maehara, S. Yamagata, N. Watanabe, S. Yuasa, Y. Suzuki and K. Ando Appl. Phys. Lett. **86** (2005) 092502.
- [8] M. Tondra, J. M. Daughton, D. Wang, R. S. Beech, A. Fink and J. A. Taylor, J. Appl. Phys. **83** (1998) 6688
- [9] K. Fujiwara, M. Oogane, F. Kou, D. Watanabe, H. Naganuma and Y. Ando, Jpn. J. Appl. Phys. **50** (2009) 122501.
- [10] A. F. Md Nor, T. Kato, S. J. Ahn, T. Daibou, K. Ono, M. Oogane, Y. Ando and T. Miyazaki, J. Appl. Phys. **99** (2006) 08T306